Journal of Thermoplastic Composite Materials
http://jtc.sagepub.com/

Effect of organic modification on the intercalation and the properties of poly(phenylene oxide)/polystyrene blend-clay nanocomposites

Rajkiran R Tiwari and Upendra Natarajan

Journal of Thermoplastic Composite Materials 2013 26: 392 originally published online 4 June 2012
DOI: 10.1177/0892705712439559

The online version of this article can be found at:
http://jtc.sagepub.com/content/26/3/392

Published by:
SAGE
http://www.sagepublications.com

Article

JOURNAL OF THERMOPLASTIC COMPOSITE MATERIAL

Journal of Thermoplastic Composite Materials
26(3) 392–415

DOI: 10.1177/0892705712439559
jtc.sagepub.com

SAGE

Effect of organic modification on the intercalation and the properties of poly(phenylene oxide)/polystyrene blend-clay nanocomposites

Rajkiran R Tiwari[1,2] and Upendra Natarajan[1,3]

Abstract

Nanocomposites prepared by the dispersion of unmodified and organically modified montmorillonite (MMT) clay into poly(2,6-dimethyl phenylene oxide)/polystyrene miscible blend in the range of 2–10 wt% clay were investigated by wide-angle x-ray diffraction, transmission electron microscopy, differential scanning calorimetry, thermogravimetric analysis and tensile mechanical tests. The systems based on unmodified sodium MMT (Na^+MMT) as well as Cloisite 20A, Cloisite 30B and Cloisite 10A organically modified clays showed polymer intercalation. The glass transition temperature (T_g) value was not affected by the volume fraction of clay and chemical nature of the organoclay. The thermal degradation stability of nanocomposites is found to be only slightly better than that of the blend matrix. A percolation threshold of around 4 wt% organoclay loading is observed. An improvement of 35% relative to unfilled polymer blend matrix is observed for the modulus, for Cloisite 20A nanocomposite containing 2 wt% organoclay. The observed modulus improvement with significant retention of elongational tensile strength and tensile ductility in case of unmodified Na-MMT and Cloisite 30B nanocomposites appears promising. The modulus prediction using Halpin-Tsai model is found to

[1] Division of Polymer Science and Engineering, National Chemical Laboratory, Pune, India
[2] Deparment of Chemical Engineering, The University of Texas at Austin, Austin, TX, USA
[3] Department of Chemical Engineering, Indian Institute of Technology, (I.I.T.) Madras, Chennai, India

Corresponding author:
Upendra Natarajan, Division of Polymer Science and Engineering, National Chemical Laboratory, Homi Bhabha Road, Pashan, Pune 411008, India.
Email: unatarajan@iitm.ac.in; u.natarajan@ncl.res.in

be closer to the experimental data when MMT volume fraction rather than the organoclay volume fraction is used.

Keywords
Polymer–matrix composites, interface/interphase, nanostructures, mechanical properties, filler

Introduction

In the past two decades, polymer–clay nanocomposites containing low-weight fraction of expandable layered silicates have gained importance due to the enhancements these materials show for bulk properties such as glass transition temperature (T_g), thermo-oxidative degradation stability, gas-permeation barrier and tensile mechanical modulus.[1–6] Sodium montmorillonite (Na-MMT) has been the most extensively used type of inorganic silicate (clay) for the investigation of the behavior of polymer nanocomposites. Typically, interfacial organic modification of MMT, using cation exchange as a viable route, is performed to render the highly polar MMT dispersible in most hydrophobic and relatively less polar polymers. The exchange of inorganic cations in the clay by organic onium ion surfactants (e.g. Quaternary ammonium type) can compatibilize the clay platelet surface with the relatively hydrophobic polymer matrix, thereby making a provision for the improvement in the wettability of clay layers with respect to the polymer matrix phase.

Intercalated and exfoliated nanocomposites show enhancement of polymer matrix properties.[1,2,4,5] Melt-processing or melt-mixing method is a viable and versatile method for nanocomposite preparation. The advantage of this method being the small preparation time and the formation of mostly intercalated and partially exfoliated nanocomposites without the requirement of solvent or other chemicals. The melt-mixing method to clay/silicate-based polymer nanocomposite has been used for a variety of engineering thermoplastics such as poly(methyl methacrylate) (PMMA),[7] polystyrene (PS),[8,9] nylon 6 and[10] polycarbonate.[11]

In the field of polymer–clay nanocomposites, relatively few studies exist especially pertaining to polymer–polymer blends.[12–36] The poly(ethylene oxide) (PEO)/polymethylmethacrylate (PMMA) organoclay nanocomposites prepared by the solvent casting have shown improved tensile mechanical modulus when compared with the polymer blend.[12] The study on the immiscible PMMA/PS blend system describes a partial level of compatibilization by organoclays as facilitated by a reduction in the size of the microdomains.[15] A substantial enhancement in the dispersion of organoclay in the polyvinylidene fluoride (PVDF) matrix was realized using PMMA as an interfacial agent at, as low as, 5 wt% in this miscible blend.[15] The dispersion of clay in this matrix resulted in an increase in shear viscosity and storage modulus. Melt-mixed PA6/PP nanocomposites prepared in the presence of maleic anhydride-*g*-polypropylene (MAH-*g*-PP) showed a significant level of property improvement due to a synergistic effect between the organoclay and MAH-*g*-PP.[16] In the immiscible poly(phenylene oxide) (PPO)/polyamide-6

(PA6) blend, the domain size of dispersed PPO phase was significantly reduced by the addition of organoclay,[20] and the matrix-domain structure was found to be transformed into a co-continuous morphology at 5 wt% clay content. Studies on the effect of organoclay on PA6/PP and PA6/acrylonitrile-butadiene-styrene (ABS) blends (at fixed composition) showed improvement in the tensile properties till 4 wt% for exfoliated cases.[21,22] The extent of exfoliation and tensile properties were found to diminish at higher clay loading. A co-continuous morphology of melt-extruded PA6/ABS nanocomposites was observed.[21] The clays were found to be exfoliated in PA6 matrix due to their better affinity toward PA6 showing improvement in mechanical properties. The polarity of the organoclay has an important role in controlling dispersed polymer phase particle size in PVDF/nylon 6 (70/30 blend) nanocomposites.[30] It was found that the organoclay (Cloisite 30B) dispersed at the interface of the immiscible blend influenced the improvement in mechanical properties when compared with the system having Cloisite 20A organoclay. The decrease in the dispersed polymer particle size and the coalescence prevention of PVDF particles leads to the formation of stiff and tough blends.

Clay nanocomposites with miscible polymer blend, as compared to a single-polymer matrix phase, have not received significant attention so far in the literature.[15,28,31,34] Recently, a study of styrene-acrylonitrile (SAN)/PMMA blend nanocomposite showed that intercalated nanocomposites are formed with commercially available Cloisite 25A MMT clay and with pristine (unmodified) MMT.[28] An insignificant increase in T_g (by 2–4°C; with unmodified MMT) and an inconsequential decrease in T_g ($\sim$1–2°C) with Cloisite 25A and Cloisite 15A was observed due to the degradation of the organic modifier at the processing temperature 230°C. In case of solution-cast IBM4VP20/SMA29 organically modified benonite nanocomposites, the dispersion quality of organoclay showed improvement with increase in SMA29 content in the blend.[34] The temperature of degradation and the T_g of the blend nanocomposite was found to increase significantly in comparison with that of the matrix. This was rationalized to be due to the presence of attractive intermolecular interactions between the clay surface and the polymer chains.

It would be interesting to consider opportunities that miscible blends offer in terms of understanding the behavior of nanocomposites and toward the design of appropriate systems with tailored properties. Recently, clay nanocomposites of miscible blend PPO/PS prepared using Cloisite 10A organoclay having phenyl groups on the quaternary cationic surfactant modifier presented sufficient clay dispersion with an improved tensile modulus.[31] In case of PPO/PS blend, both the polymers PPO and PS are amorphous and molecularly miscible as observed in various characterization techniques such as optical microscopy, calorimetry and electron microscopy.[37–39] The van der Waals and dipolar interactions between phenyl groups of PPO and PS give miscibility at the molecular level in this blend.[40] PS is brittle, while PPO is a ductile plastic. Hence, the blend exhibits a characteristic property from brittle material to ductile material and composition-dependent mechanical properties. PPO along with PS exhibits a broad range of outstanding properties for applications in computers and business equipment, in automotive industry, for electrical insulation, in telecommunications, electronics and many other industries.[41] The mechanical strength, thermal stability and flame retardancy are desirable properties for machine and appliance housings.

The objective of the present study is to investigate the effect of organic modification versus unmodified MMT clay for nanocomposite formation, glass transition (T_g), thermal degradation behavior and tensile mechanical properties of PPO/PS nanocomposites. Commercially available Noryl sample system with a fixed PPS/PPO composition was chosen for this investigation. The influence of organic modification and the comparison of the performance of organically modified and unmodified MMT for this blend are not available in the literature. The nanocomposites were prepared using melt-processing method and characterized using wide-angle x-ray diffraction (WAXD), transmission electron microscopy (TEM), differential scanning calorimetry (DSC), thermogravimetric analysis (TGA) and mechanical tensile tests.[7,31,42,43] These properties were studied in 2–10 wt% range of either Na^+MMT or the organically modified clays (in which case the MMT filler amount was different at the same organoclay loading across the different organoclays).

Experimental

Materials

Na-MMT and organically modified clays were supplied by Southern Clay Products Inc. (Gonzales, TX, USA) in powder form. Cloisite® Na (MMT), a natural Na-MMT with cation exchange capacity (CEC) 92.6 mequiv/100 g was used as is without further modification. The organically modified clays used included Cloisite 10A (C10A) having dimethyl benzyl hydrogenated tallow quaternary ammonium as an organic modifier with a CEC value of 125 meq/100 g, Cloisite 30B (C30B) having methyl tallow bis-2-hydroxyethyl quaternary ammonium with a CEC value of 90 meq/100 g and Cloisite 20A having dimethyl ditallow quaternary ammonium with a CEC value of 90 meq/100 g. Here, HT or MT refers to hydrogenated tallow or tallow as be the source; however, the aliphatic tail length is a mixture of C14, C16 and C18 (65% by mol.) consistently in all three types of modifier molecules. For upto a difference of ± 5 meq/100 g in the CEC value, the number of organic modifier cations per lattice unit cell of MMT clay would not differ by an integer, and therefore, the density of the modifiers on the ion-exchanged MMT surface of Cloisite 20A and Cloisite 30B or on the unmodified Cloisite Na-MMT would be the same. Cloisite 10A presents an overexchanged organoclay with the density of the modifier molecules being higher than that of the exchangeable Na^+ ions. Therefore, in this clay, there is propensity for the organic modifiers to diffuse out of the interlayer space into the polymer matrix and act as diluents in the course of nanocomposite preparation at temperatures used in this study. Given the much lower density of organic modifier compared with silicate MMT, the differences in the molecular weights and CEC across the systems would not present a significant difference in the weight fraction of silicate across these organoclays for a fixed value of the organoclay loading. Therefore, mechanical properties were assessed on the basis of actual organoclay loading instead of silicate (MMT clay) loading. The exception being Cloisite 10A systems, wherein the excess organic surfactant (given 125 meq/100 g overexchanged concentration compared with 90 meq/100 g CEC value of the original unmodified Na^+MMT) would leach out of the interlayer spacing

during the processing of the hybrids and results in a reduction in the mechanical properties of the matrix phase of the nanocomposite (effectively, for the nanocomposite itself). The PPO/PS blend commercial sample grade Noryl 701 supplied by General Electric was obtained in the form of pellets and used as is without further modification.

Nanocomposite preparation

The blend samples and clays were dried at 110°C and 80°C, respectively, in an air circulatory oven for a time period of 8 h prior to mixing. The blend and required amount of organoclay (2, 4, 6, 8 and 10 wt%) were physically mixed in a glass beaker and further melt-blended in a Haake Rheocord® batch mixer (Waltham, MA, USA) (50 g scale) originally at 220°C, as test condition, which is a typical processing temperature for PPO/PS blend.[31] However, for the purpose of investigating a suitable lower processing temperature, in order to avoid degradation of organic modifier moieties, the samples were processed at 180°C successfully.[31] WAXD data for the organoclay systems in the present study as well as earlier study revealed the degradation of organic modifier at the higher processing temperature.[31] Therefore, lower processing temperature of 180°C was used for conducting the further study. The mixing speed and processing time were fixed at 60 r/min and 15 min, respectively, as these conditions are optimized from earlier studies on PMMA and PS nanocomposites processed in the range of 20–75 r/min.[7,31,42,43] The d_{001} spacing of the clay layers in the nanocomposites were found to be constant beyond 15 min of mixing time. The maximum change Δd_{001} spacing was observed for the hybrids prepared at 60 r/min.[31] The approximate composition of the blend was determined using Flory-Fox equation and the measured T_g value.[37]

Characterization

Wide angle x-ray diffraction. The intercalation of PPO/PS molecularly compatible (miscible) blend in between the clay layers was confirmed using WAXD. The WAXD patterns were recorded on a Rigaku (Japan) diffractometer with CuKα radiation (wavelength $\lambda = 1.5418$ Å) at 40 kV and 100 mA. The experiments were performed on compression-molded films in a scan range of $2\theta = 2°$–$14°$ with a step size of 0.05 and scan speed of 2° per min. The scan speed range of 0.5°–5° per min for nanocomposites has been typically used in literature.[44,45] The selected scan speed of 2° per min is found to be sufficient to cover all data points. Too low a scan rate consumes unnecessary time, while too high a rate increases noise in the curve without improving the feature derivation in keeping with requirements posed by these intercalated samples.

Transmission electron microscopy. Ultrathin sections of approximately 50–70 nm were cut with a diamond knife at room temperature with a Leica Ultracut UCT® microtome (Vienna, Austria). Sections were collected on 300 mesh carbon-coated copper grids and dried on filter paper overnight. TEM imaging was performed using a JEOL 1200EX electron microscope (Tokyo, Japan) operating at an accelerated voltage of 80 kV. Images

were captured using charged couple detector camera and images were viewed using Gatan® digital micrograph software. The procedures followed were per the standard ones in the literature, which are similar to earlier investigations.[31,42,43]

Thermal characterization. T_g measurements were performed using Perkin Elmer DSC-7 (Waltham, MA, USA) differential scanning calorimeter per the standard procedure used earlier.[7,31,42,43] Calibration was done using indium and sapphire as standards and nitrogen flow through the DSC cell was maintained at 20 mL/min. The furnace was heated till 600°C and kept for 10 min to remove impurities. Heat–quench cycles were in the range of 50–170°C. Samples of 5–10 mg were measured in an aluminum pan (40 μL capacity). Quench rate of 50°C/min was used in the cooling part of the cycle. The data obtained from the second heating scan was used to determine the T_g value.[7,31]

The onset of degradation as the temperature at 1 wt% loss (T_1), at 5% weight loss (T_5) and at maximum degradation rate (T_{max}) was determined using Perkin Elmer TGA-7 (Waltham, MA, USA) instrument per the earlier procedures.[7,31] Samples of 5–10 mg were heated from 50°C to 700°C at 10°C/min under nitrogen atmosphere. Nitrogen flow rate was fixed at 20 mL/min. A heating rate of 10°C/min was selected to maintain accuracy of data and to get smooth TGA curves.[46] The T_{max} value, determined from the peak position of DTG curve, was obtained from the TGA curve using Pyris® software (Shelton, CT, USA) interfaced with the equipment. Experiments were performed on three samples for each system.

Mechanical characterization and testing. Tensile properties of the nanocomposites were determined using rectangular strips prepared by compression molding, per procedure used earlier.[31] The PPO/PS nanocomposites could not be injection molded using known conditions for typical thermoplastics and this blend, due to their significantly high melt viscosity. Hence, rectangular strips were cut from the compression molded nanocomposite sheet. Films were prepared by compression at 185°C for 5 min using electrically heated Carver® press, and the hot plates were cooled using water circulation. The dimensions of the strips were 150 × 12 × 0.8 mm^3. Compression molding parameters were optimized to get uniform sheets without any defects. The rectangular strips were obtained from the compression molded sheet using metal sheet cutter machine, and samples with smooth edges and without defects were selected for test.

The standard ASTM D882 test method typically used for thin plastic sheets with the thickness of <1 mm was used. The width/thickness ratio in this test method should be at least 8 and is ~15 in the present cases. The Young's modulus, the break stress (tensile strength at break) and the break strain (%) were determined using INSTRON® 4204 universal testing machine (Norwood, MA, USA) with 1 kN load cell. Grip separation was used as the means by which the strain was measured. The initial grip distance was 120 mm and the crosshead speed was maintained at 5 mm/min. All tests were performed at room temperature and 50% relative humidity. The data reported in all the cases for all the samples are the average of 10 independent measurements with standard deviations. Proper care was taken in selecting samples for the test, as in some cases, especially for Cloisite

Table 1. d-Spacing values (nm) for PPO/PS blend nanocomposite samples processed and prepared at 180°C.

	Clay loading (wt%)				
System	2	4	6	8	10
PPO/PS-Na-MMT d001 (nm)	1.5	1.4	1.5	1.5	1.5
Δd^a (nm)	0.2	0.2	0.2	0.2	0.2
PPO/PS-C10A d001 (nm)	2.9	3.1	3.0	2.9	3.0
Δd (nm)	0.9	1.2	1.1	0.9	1.1
PPO/PS-C30B d001 (nm)	3.2	3.4	3.2	3.3	3.3
Δd (nm)	1.3	1.5	1.3	1.4	1.4
PPO/PS-C20A d001 (nm)	3.1	3.4	3.0	3.3	3.0
Δd (nm)	0.6	0.9	0.5	0.8	0.5

PPO: poly(phenylene oxide); PS: polystyrene.
[a] Δd (nm) = difference between basal spacing of composites and clay.

10A-based systems, samples had to be prepared at least twice in order to obtain visually clear and macroscopically homogeneous molded sheet.

Results and discussion

Nanocomposite structure

The hybrids prepared at 220°C (the usual processing temperature for PPO/PS blend) clearly showed degradation of the organic modifier, similar to the observation made in the earlier study.[31] Under these mixing conditions, the depreciation (reduction) in the d_{001} spacing (data not shown specifically here) for different chemical systems was in the range of 0.3–0.5 nm over 2–8 wt% organoclay loading. By lowering the processing temperature to 180°C, the melt was easily formed within few minutes at 60 rpm, followed by a mixing time of 10 min. WAXD results (d_{001}) for PPO/PS composites processed at 180°C are given in Table 1. The lower processing temperature results in intercalated nanocomposites without the degradation of the organic modifiers. This was confirmed by weight measurements via TGA (Table 2).

As seen in Figure 1 for unmodified Na-MMT-based hybrids, the nanocomposites reach the peak at 1.5 nm when compared with 0.9 nm for dehydrated Na^+MMT and 1.3 nm for hydrated-Na^+MMT. This shows polymer intercalation between the silicate layers. It can be inferred that PPO chains have intercalated into Na^+MMT layers. It is known that PS does not intercalate into unmodified Na-MMT, while alkyl ammonium quaternary ion–modified MMT does promote intercalation.[8,47] This was also observed by our independent experiments on the PS-MMT system not reported here.

As shown in Figure 2 for Cloisite 30B-based nanocomposites, the shifts of the x-ray diffraction (XRD) peaks toward lower 2θ values confirm polymer intercalation. The nanocomposite peaks are relatively broader at 2 wt% clay loading. This shows better

Table 2. Comparison of thermal degradation properties.

System	Clay (wt%)	Temperature[a] (°C)		
		$T_{1\%}$	$T_{5\%}$	T_{max}
PPO/PS	0	282	396	445
PPO/PS-CNa	2	254	391	445
	6	218	388	455
	10	254	392	448
PPO/PS-C10A	2	307	415	464
	6	238	365	464
	10	300	404	464
PPO/PS-C20A	2	306	415	462
	6	239	365	469
	10	300	404	465
PPO/PS-C30B	2	293	405	447
	6	254	379	453
	10	254	375	456

PPO: poly(phenylene oxide); PS: polystyrene; TGA: thermogravimetric analysis.
[a] T_1 and T_5 are the temperatures determined from TGA analysis at 1% and 5% weight loss of organic content in nanocomposites. T_{max} gives the temperature pertaining to the maximum rate of weight loss as determined from DTG curve.

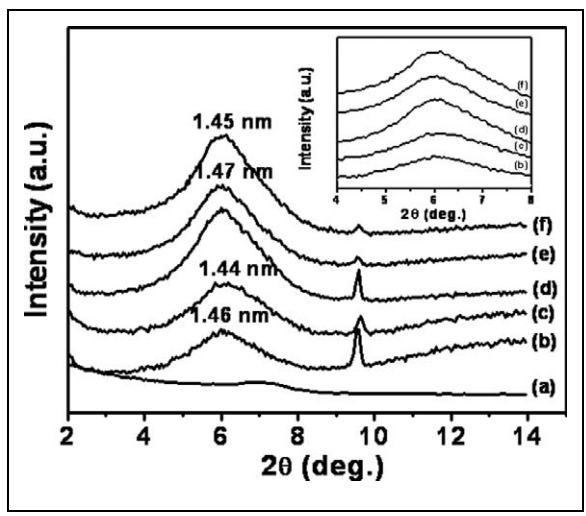

Figure 1. WAXD curves of PPO/PS-Na-MMT nanocomposites as a function of organoclay loading. (a) CloisiteNa clay, (b) 2 wt%, (c) 4 wt%, (d) 6 wt%, (e) 8 wt% and (f) 10 wt%. The d001 peak for montmorillonite CloisiteNa clay is not sharp as portrayed here, given the rescaling of intensity to relative measure for the purpose of plotting all systems on a common graph. Value of d001 peak for Na^{+}MMT clay occurs at $2\theta = 7.2$ Å. WAXD: wide-angle x-ray diffraction; PPO: poly(phenylene oxide); PS: polystyrene; Na-MMT: sodium montmorillonite.

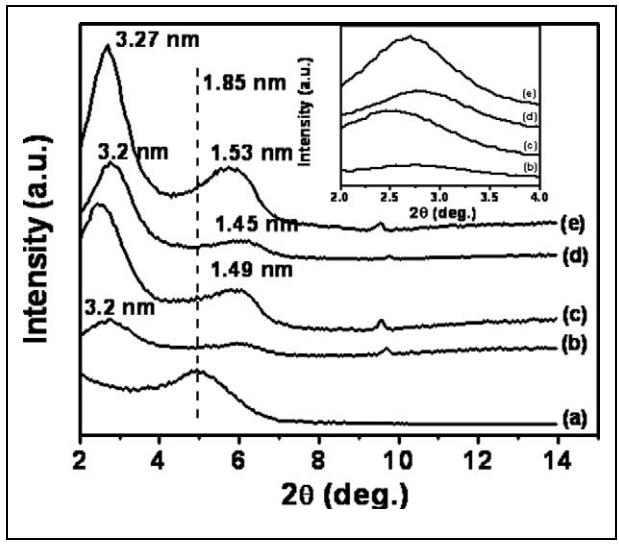

Figure 2. WAXD curves of PPO/PS-Cloisite 30B nanocomposites as a function of organoclay loading. (a) Cloisite 30B organoclay, (b) 2 wt%, (c) 4 wt%, (d) 6 wt%, (e) 8 wt% and (f) 10 wt%. Dashed vertical line shows the location of the organoclay d001 peak. WAXD: wide-angle x-ray diffraction; PPO: poly(phenylene oxide); PS: polystyrene.

dispersion for lower clay fraction. Cloisite 30B organoclay contains methyl tallow bis(2-hydroxyethyl) quaternary ammonium ions which, being relatively polar, forms thermodynamically favorable interactions with PPO chains, resulting in polymer intercalation. At higher clay loading, the clay tactoids show well-ordered multilayer structure with polymer intercalation. The change Δd_{001} is in the range of 13–15 Å. The hydroxyl groups present in Cloisite 30B organic modifier facilitates favorable interactions between the clay and the PPO and the PS chains of the blend matrix.

As seen from Figure 3 for PPO/PS–Cloisite 10A hybrids (lower loadings given in earlier work[31]), sufficient polymer intercalation is observed even at higher loadings (8 and 10 wt%). The intercalation change Δd_{001} is found to vary in the range of 0.9–1.5 nm. Cloisite 10A contains dimethyl benzyl hydrogenated tallow quaternary ammonium modifier. The presence of the benzyl ring (due to dipolar interactions) in this modifier improves the thermodynamic compatibility between the organoclay and PS chains.[48,49] The Δd_{001} value reported in the literature for PS–Cloisite 10A intercalated nanocomposite is in the range of 4.0–4.9 nm depending on the PS molecular weight and clay loading, as obtained by the use of higher shear in the specific twin-screw extruder configuration used.[49] If the excess organic modifier was not present (i.e. washed off chemically prior to the use of organoclay in melt-mixing with the PPO/PS blend), then a larger change in Δd_{001} value would have been observed for the same final value of the nanocomposite d001. This confirms the earlier observation made on PS homopolymer system intercalated into cationic phosphonium and

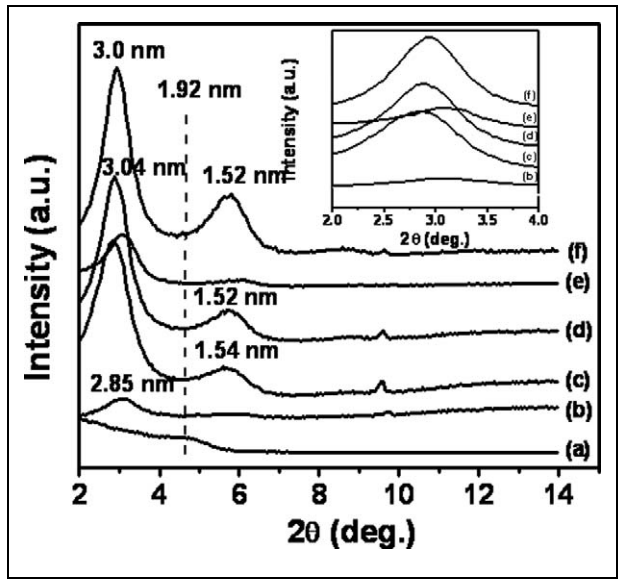

Figure 3. WAXD curves of PPO/PS-Cloisite 10A nanocomposites as a function of organoclay loading. (a) Cloisite 10A organoclay, (b) 2 wt%, (c) 4 wt%, (d) 6 wt%, (e) 8 wt% and (f) 10 wt%. Dashed vertical line shows the location of the organoclay d001 peak. Data for systems (a) to (c) are reproduced from Wiley, 2008.[31] WAXD: wide-angle x-ray diffraction; PPO: poly(phenylene oxide); PS: polystyrene.

quaternary ammonium based (containing polar-substituted aromatic ring) on excess quantities that lessened the tendency of PS chains to penetrate the organoclay during melt processing,[50] likely due to blockage presented by the excess modifier between successive clay platelet layers.

Figure 4 shows the WAXD patterns for PPO/PS–Cloisite 20A nanocomposites. The value of Δd_{001} change obtained due to polymer intercalation is lower than that seen in the nanocomposites with the other two organoclays. This is likely due to the very hydrophobic nature of the organic modifier in this organoclay. The largest value of Δd_{001} in the Cloisite 20A nanocomposite occurs at the same clay loading (4 wt%) at which the best improvement in tensile modulus is observed, and this shows the percolation threshold observed in this system.

The difference seen in Δd_{001} between Cloisite 10A and Cloisite 30B systems, in going from organoclay to the polymer-intercalated nanocomposite, even though these contain organic modifier molecules of similar size and not too dissimilar polarity, can be rationalized by the fact that Cloisite 10A contains excess modifier, which if were washed away prior to nanocomposite formation should give similar d-spacing change as Cloisite 30B. Similarly, it should be noted that interlayer spacing increases in a step-wise manner in alkyl ammonium–modified MMTs as more longer alkyl substituents are added to the modifier molecule, consistent with the formation of a modifier

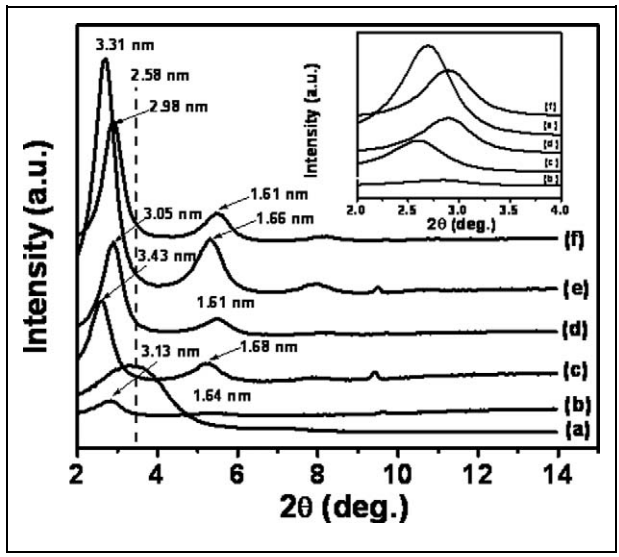

Figure 4. WAXD curves of PPO/PS-Cloisite 20A nanocomposites as a function of organoclay loading. (a) Cloisite 20A organoclay, (b) 2 wt%, (c) 4 wt%, (d) 6 wt%, (e) 8 wt% and (f) 10 wt%. Dashed vertical line shows the location of the organoclay d001 peak. WAXD: wide-angle x-ray diffraction; PPO: poly(phenylene oxide); PS: polystyrene.

monolayer, then a bilayer, and so on. Cloisite 30B and Cloisite 10A do not contain quite enough alkyl chains in the interlayer galleries to initiate the formation of the next monolayer whereas Cloisite 20A does. The addition of polymer would be expected to cause a large increase in d-spacing in the Cloisite 30B and Cloisite 10A cases than in Cloisite 20A case, even if the final d-spacings are similar in all cases.

TEM images are shown in Figure 5. As seen in Figure 5(a) clay tactoids are visible in the unmodified MMT system, suggesting the formation of a dispersed microcomposite rather than a nanocomposite. As seen in Figure 5(b) to (d) for intercalated nanocomposites, the dispersion of clay layers appears to be slightly better at 2 wt% (low loading) supported by the WAXD data, wherein low intensity and slightly broader peaks are observed for systems at 2 wt% when compared with those at 10 wt%. The TEM images at higher loadings show the presence of clay stacks and tactoids.

It is worth mentioning here that at present no consistent behavioral trend in particular can be ascribed to the role of the excess organic modifier toward the development of the nanocomposite structure, as observed from literature restricted to melt-processed nanocomposites. A more open (separated) organoclay structure due to the excess surfactant could enhance exfoliation during nanocomposite synthesis[51,52] or could improve mechanical properties of a poly(ethylene-*co*-methacrylic acid) ionomer beyond that observed with the stoichiometric organoclay[53] or that the best properties of polyethylene and poly(ethylene-*co*-vinyl acetate) could be occurred[54] when the organoclay contained 20–50% excess surfactant or that excess modifier was required for the intercalation of PP

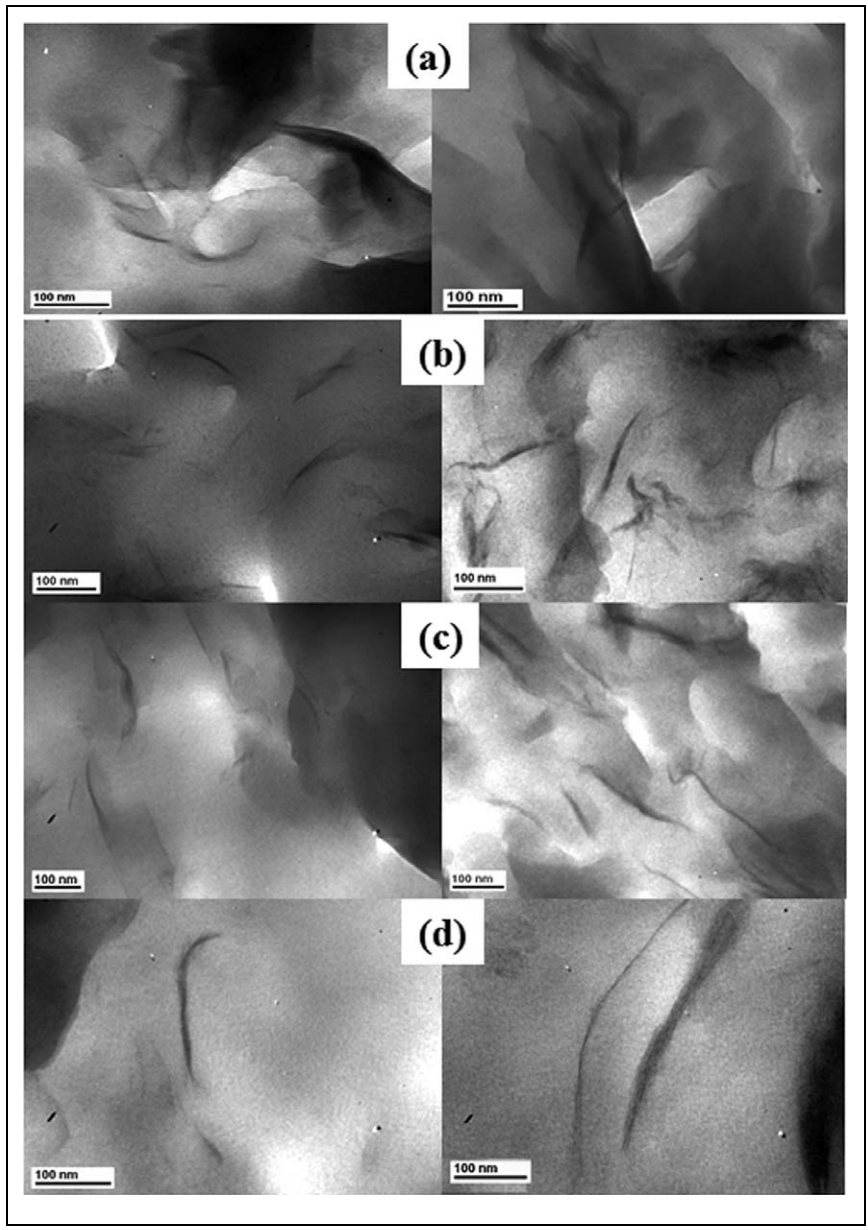

Figure 5. High-magnification TEM images of PPO-PS blend clay nanocomposites. Left-side images are for 2 wt% and right-side images are for 10 wt% clay except for C20A (4 wt%). (a) Na-MMT-based nanocomposite, (b) Cloisite 10A-based nanocomposite (image for 2 wt% loading taken from Wiley, 2008,[31] (c) Cloisite 20A-based nanocomposite and (d) Cloisite 30B-based nanocomposite. TEM: transmission electron microscopy; PPO: poly(phenylene oxide); PS: polystyrene; Na-MMT: sodium montmorillonite.

into the organoclay tactoids during extrusion accompanied with a decrease in the quality of the tactoid dispersion assessed by TEM[52] and that approximately 30% excess organic surfactant (quaternary ammonium salt) in an organoclay reduced the ease of platelet dispersion in melt-extruded nylon 6 nanocomposites.[10] In this context, the excess organic modifier present in Cloisite 10A organoclay used with PPO/PS blend does not make a significant difference in the polymer intercalation; however, the other organoclays are found to give better modulus and better retention (less decrease) of tensile strength at organoclay loadings upto 4 wt% in the nanocomposite, as discussed in the later section on the mechanical properties.

Glass transition and thermal degradation behavior

DSC data revealed that hybrids for all systems showed glass transition, but clay loading and confinement due to intercalation did not have a significant effect on the transition temperature. The CloisiteNa composites revealed approximately 5°C change in T_g (117–123°C), which is only a slight improvement on the organically modified clay systems. The T_g of PPO/PS blend is 117°C.[31] These results are similar to those seen from earlier studies on intercalated PS nanocomposites, which did not show change in the matrix T_g in the presence of MMT clay.[3,55,56] For samples prepared with Cloisite 30B organoclay, the T_g value is relatively lower at higher clay loading values. As evident from the literature on polymer–clay nanocomposites, either a decrease or an increase in T_g has been observed, which depends on the state of dispersion, and the chemical structures of the polymer and organic modifier molecules. While PS nanocomposites prepared by melt-processing method do not show any appreciable enhancement or variation in T_g, the nanocomposites prepared via in situ polymerization route do show relatively different results.[57,58] The behavior of T_g is in specific to the particular polymer matrix in consideration.

TGA results are presented in Figure 6. It is known that T_{10} value levels off beyond 3 wt% MMT clay for the PS nanocomposite prepared by in situ polymerization method.[59] The hybrids in the present study show little improvement in degradation behavior as seen by the results for T_1, T_5 and T_{max}. No unusual trends were observed as a function of organoclay loading across the chemically different systems.

Tensile properties

The Young's modulus, tensile strength and tensile break strain data are presented in Tables 3 to 5 and Figure 7. Depending on the type of organoclay, the improvement in the modulus is 11–31%, with the lowest value pertaining to that for the weakly intercalated PPO/PS–Na-MMT hybrid and the highest value is obtained for the Cloisite 30B nanocomposite beyond 6 wt%. Such increase in modulus has been previously observed for melt-processed thermoplastic nanocomposites of 3–69% for PMMA,[42,43] 4–24% for PS[9] and 25–66% for SAN[60] over 2–10 wt% MMT filler.

The intercalated nanocomposites and the composites show modulus enhancement as compared to the blend (modulus 2.49 GPa) at the lowest loading value (i.e. 2 wt%). All

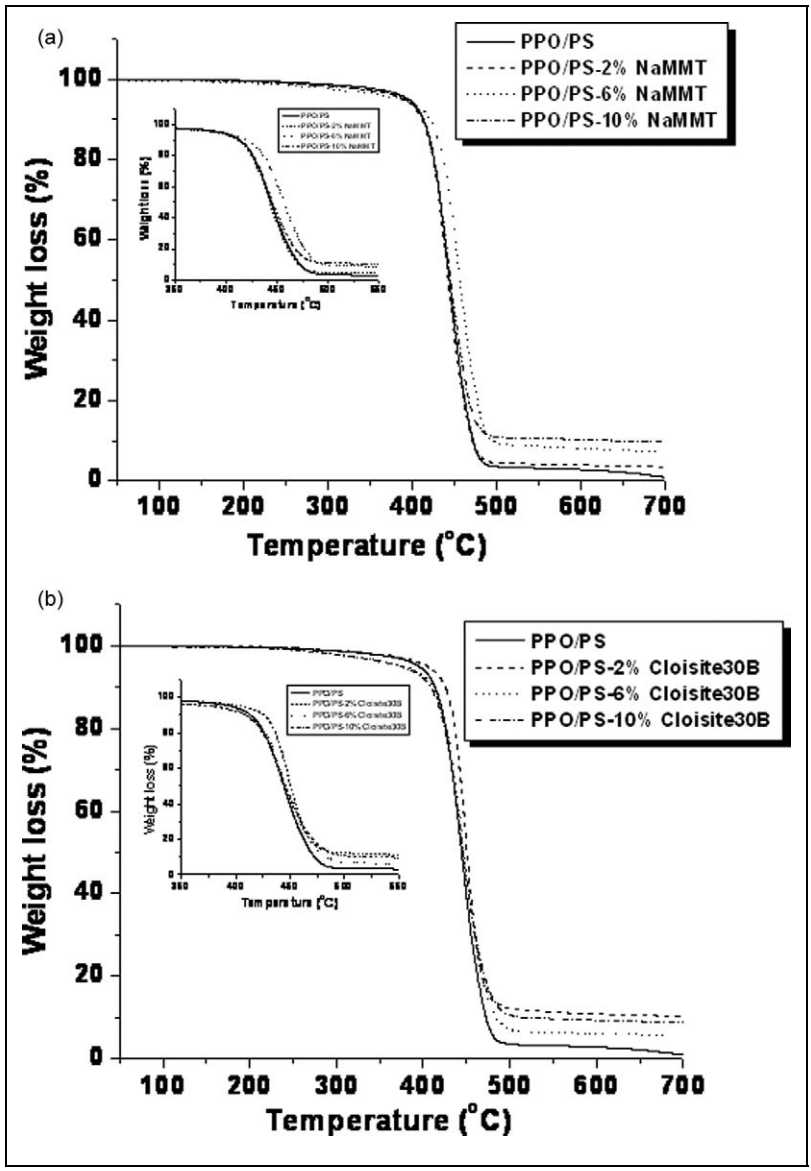

Figure 6. TGA thermographs; (a) PPO/PS-Na-MMT and (b) PPO/PS-Cloisite 30B. TGA: thermogravimetric analysis; PPO: poly(phenylene oxide); PS: polystyrene; Na-MMT: sodium montmorillonite.

three organoclays give sufficient enhancement in the modulus. The Cloisite 20A-based systems showed significant loss of modulus at higher loading values; a behavior that is seen to be unusual and the understanding of which is beyond the scope of the present work. It is likely that in this particular system, clay loadings beyond the percolation

Table 3. Young's modulus (*E*; GPa) of PPO/PS blend and nanocomposites.

	Young's modulus[a] (*E*; GPa)				
	Clay loading				
System	2 wt%	4 wt%	6 wt%	8 wt%	10 wt%
PPO/PS-CNa	2.8 ± 0.2	2.9 ± 0.1	2.8 ± 0.1	2.8 ± 0.1	3.1 ± 0.1
PPO/PS-C10A	2.9 ± 0.2	3.2 ± 0.1	3.3 ± 0.1	–	–
PPO/PS-C30B	3.0 ± 0.2	3.2 ± 0.2	3.2 ± 0.2	3.2 ± 0.1	–
PPO/PS-C20A	3.3 ± 0.1	2.8 ± 0.1	2.4 ± 0.1	2.5 ± 0.2	2.8 ± 0.1

PPO: poly(phenylene oxide); PS: polystyrene.
[a] Modulus of unfilled blend is 2.5 ± 0.2 GPa.

Table 4. Break stress (σ_{brk}; MPa) of PPO/PS blend and nanocomposites.

	Break stress[a] (σ_{brk}; MPa)				
	Clay loading				
System	2 wt%	4 wt%	6 wt%	8 wt%	10 wt%
PPO/PS-CNa	37.6 ± 2.5	37.1 ± 1.3	37.3 ± 2.1	36.6 ± 1.9	40.9 ± 2.3
PPO/PS-10A	22.0 ± 2.4	40.0 ± 2.4	18.4 ± 4.5	–	–
PPO/PS-30B	40.3 ± 3.2	40.2 ± 2.8	41.2 ± 3.4	35.5 ± 2.8	–
PPO/PS-20A	47.4 ± 1.4	38.5 ± 2.2	26.7 ± 2.4	24.5 ± 1.7	39.5 ± 1.8

PPO: poly(phenylene oxide); PS: polystyrene.
[a] Break stress of unfilled blend is 50.8 ± 2.2 MPa.

Table 5. Break strain ($\in_{brk}$; %) of PPO/PS blend and nanocomposites.

	Break strain[a] ($\in_{brk}$; %)				
	Clay loading				
System	2 wt%	4 wt%	6 wt%	8 wt%	10 wt%
PPO/PS-CNa	2.2 ± 0.1	2.1 ± 0.1	2.1 ± 0.2	2.1 ± 0.2	1.8 ± 0.2
PPO/PS-C10A	1.1 ± 0.1	1.6 ± 0.2	0.8 ± 0.1	–	–
PPO/PS-30B	2.2 ± 0.2	1.7 ± 0.1	1.8 ± 0.2	1.0 ± 0.1	–
PPO/PS-C20A	2.3 ± 0.1	2.0 ± 0.1	1.4 ± 0.2	1.3 ± 0.1	2.1 ± 0.1

PPO: poly(phenylene oxide); PS: polystyrene.
[a] Break strain of unfilled blend is 3.6 ± 0.17.

threshold (seen at 4 wt% organoclay) lead to poorly structured composites. Cloisite 10A-based nanocomposites at 8 and 10 wt% organoclay loading were very brittle to be tested on the INSTRON.

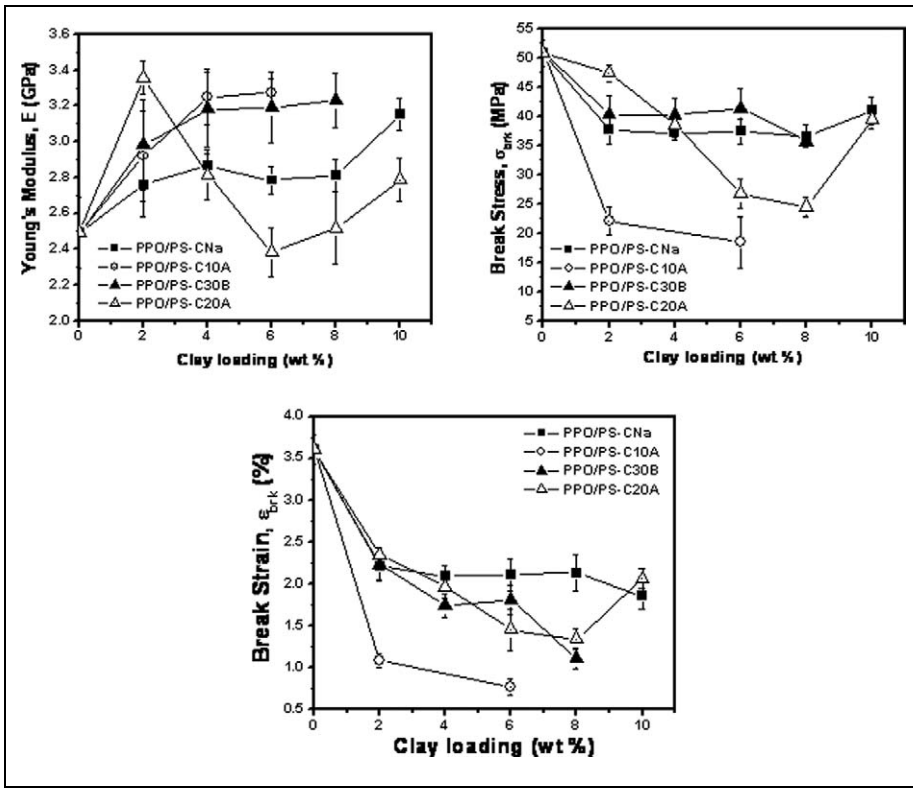

Figure 7. Variation in the mechanical properties of PPO/PS blend nanocomposite. PPO: poly(phenylene oxide); PS: polystyrene.

The Young's modulus of nanocomposite was calculated from Halpin-Tsai theory. The aspect ratio of clay stack were calculated using stack thickness as determined from Scherrer equation and stack length from TEM image using Gatan digital micrograph software (Warrendale, PA, USA). The variation in aspect ratio with clay loading was not significant so as to affect the modulus significantly. The Halpin-Tsai theoretical model was used to predict the stiffness of these nanocomposites as a function of the aspect ratio of the clay filler particles within the polymer blend matrix. The results of the calculation are given in Table 4 using structural parameters listed in Table 3 as obtained from the experiments discussed in this study. The number of clay platelets per stack in the nanocomposite samples was determined using the Scherrer equation with the data on d_{001} (*d*-spacing) as obtained from the WAXD curves. The average stack length (longest dimension of the clay stack which would be the lateral dimension of the clay platelets) was measured from TEM images with at least 150–180 counts taken for each clay loadings. The stack length was measured at 2 and 10 wt% clay loading and the particle length was found to be fairly constant for the clay loading range

Table 6. Tensile modulus and parameters for PPO/PS nanocomposites.

System	Clay loading (wt%)	MMT (wt%)	Organoclay (vol %)	AR[a]	Modulus, *E* (experiment; GPa)
PPO-PS-CNa	2	2.00	0.75	10.83	2.76 ± 0.18
	4	4.00	1.51	10.83	2.86 ± 0.07
	6	6.00	2.29	10.83	2.78 ± 0.08
	8	8.00	3.10	10.83	2.81 ± 0.09
	10	10.00	3.93	10.83	3.15 ± 0.10
PPO-PS-C10A	2	1.23	0.46	17.16	2.92 ± 0.25
	4	2.48	0.93	9.84	3.21 ± 0.14
	6	3.75	1.41	9.88	3.27 ± 0.07
	8	5.04	1.91	13.58	–
	10	6.35	2.43	13.14	–
PPO-PS-C30B	2	1.41	0.52	16.32	2.98 ± 0.25
	4	2.83	1.06	18.12	3.18 ± 0.21
	6	4.28	1.62	15.85	3.19 ± 0.2
	8	5.74	2.19	15.11	3.23 ± 0.15
	10	7.22	2.78	–	–
PPO-PS-C20A	2	1.25	0.46	13.75	3.35 ± 0.09
	4	2.52	0.94	10.82	2.81 ± 0.14
	6	3.81	1.43	10.23	2.38 ± 0.14
	8	5.12	1.94	9.97	2.52 ± 0.20
	10	6.44	2.47	9.14	2.78 ± 0.12

PPO: poly(phenylene oxide); PS: polystyrene; MMT: montmorillonite.

[a] The aspect ratio for PPO/PS-CNa is considered constant at all clay loadings, given the lack of polymer intercalation.

studied discussed in this study. The calculation of the volume fraction of the intercalated material is based on the interlayer spacing within the silicates stack and is obtained as the ratio of the total gallery stack thickness over the stack thickness based solely on MMT silicate layers (i.e. devoid of intercalated polymer chains and organic modifier). The modulus values for MMT and PPO/PS blend were taken as 178 GPa (value for Na-MMT) and 2.49 GPa, respectively (experimentally measured here). Using these parameters, the modulus of the nanocomposites was calculated by the Halpin-Tsai equation. The parameters used and the results of the calculations are given in Tables 6 and 7. The absolute comparison of the modulus between those predicted by the Halpin-Tsai model and the experimentally measured values is not good, except for the Cloisite 10A systems upto 6 wt% loading.[31] The Halpin-Tsai model prediction is found to be closer to the experimental data when the MMT volume fraction is used rather than the organoclay volume fraction.

The depreciation in the break stress (as compared to neat blend matrix) of 19–64%, the lower value being for the Cloisite 30B nanocomposites as better than the Cloisite 10A nanocomposites investigated here and in earlier work.[31] The break strength for the systems based on CloisiteNa and Cloisite 30B does not depreciate significantly. In

Table 7. Compilation of structural parameters and Young's modulus determined experimentally and obtained by Halpin-Tsai model.[a]

System	d_{001} (Å)	Volume fraction[a]		No. of platelets N_c (integral)	$E_{expt.}$ (GPa)	$E_{H\text{-}T}$[b] (GPa)	$E_{H\text{-}T}$[c] (GPa)
		ϕ_{OC}	ϕ_{MMT}				
PPO/PS	–	0	0	–	2.49	2.49	2.49
C-Na (2%)	15	0.0075	0.0046	3.4	2.76	2.76	2.67
C-Na (4%)	14	0.0151	0.0093	3.2	2.86	3.09	2.86
C-Na (6%)	15	0.0229	0.0141	3.5	2.78	3.39	3.04
C-Na (8%)	15	0.0310	0.0191	3.9	2.81	3.72	3.24
C-Na (10%)	15	0.0393	0.0243	4.0	3.15	4.05	3.45
C10A (2%)	29	0.0107	0.0075	3.6	2.92	2.88	2.78
C10A (4%)	31	0.0216	0.0151	5.2	3.21	3.11	2.91
C10A (6%)	30	0.0326	0.0229	5.2	3.27	3.41	3.15
C10A (8)	29	0.0439	0.0310	4.3	–	4.05	3.58
C10A 10%)	31	0.0555	0.0393	4.2	–	4.38	3.83
C30B (2%)	32	0.0107	0.0046	3.3	2.98	2.88	2.66
C30B (4%)	34	0.0217	0.0094	2.9	3.18	3.32	2.85
C30B (6%)	32	0.0328	0.0143	3.4	3.19	3.70	3.01
C30B (8%)	33	0.0442	0.0194	3.4	3.23	4.06	3.18
C30B (10%)	33	0.0557	0.0247	–	–	–	–
C20A (2%)	31	0.0120	0.0052	4.1	3.35	2.90	2.67
C20A (4%)	34	0.0242	0.0106	4.6	2.81	3.18	2.79
C20A (6%)	30	0.0366	0.0162	5.3	2.38	3.55	2.96
C20A (8%)	33	0.0491	0.0219	5.1	2.52	3.88	3.10
C20A (10%)	30	0.0619	0.0278	5.8	2.78	4.22	3.25

PPO: poly(phenylene oxide); PS: polystyrene.

[a] Volume fraction of organoclays and montmorillonite in nanocomposites.

[b] Young's modulus determined from Halpin-Tsai theory (with organoclay volume fraction).

[c] Young's modulus determined from Halpin-Tsai theory (with Montmorillonite volume fraction).

comparison, the Cloisite 10A nanocomposite system shows lower tensile strength likely due to the presence of excess surfactant (organic modifier). This is due to the presence of the excess organic modifier in Cloisite 10A over and above the stoichiometric amount. The minimum decrease in comparison with blend in percentage (loading in parenthesis) for each clay system was as follows: 26 (2 wt% for PPO/PS-CloisiteNa), 21 (4 wt% for PPO/PS-Cloisite 10A), 19 (6 wt% for PPO/PS-Cloisite 30B) and 6.7 (2 wt% Cloisite 20A). The effect of organic modifier and clay loading on break strength in PPO/PS blend nanocomposite corroborate with reported results for intercalated SAN nanocomposite,[60] except for the much lower value of break strength seen for Cloisite 10A system in the present study.

In the context of polymer-filler nanocomposite, in particular, it is known that the tensile strength for thermoplastic and thermoplastic blend nanocomposites reduces with clay loading.[9,31,42,43,61] The filler–filler interaction and inter-filler interaction causes clay particles to agglomerate, leading to a reduction in strength.[62] Bigg found increase

in tensile strength for Noryl-talc composite, while tensile strength reduced for ABS-talc, with increase in talc composition, and this behavior was attributed to greater affinity of Noryl for talc arising from the presence of a coupling agent used with talc.[63] Leong et al. have shown either an increase or slight decrease in tensile strength of PP composites prepared with various inorganic fillers. The increase in the tensile strength was mainly due to the good filler–matrix interactions, which were largely due to the platy nature of talc and kaolin as compared to $CaCO_3$.[64] The various factors such as matrix, crystallinity and filler type can have a significant effect on the tensile strength. More recent seminal literature on PP-clay nanocomposites[65,66] brings out the complex interplay between processing, microstructure (crystalline and noncrystalline fractions) and mechanical properties that needs to be understood in general for prediction and design of hybrid materials such as these for engineering applications.

The break strain ($\in_{brk}$) of the nanocomposites studied in the present work is found to decrease with an increase in the clay loading. This qualitative trend is sufficiently general for brittle thermoplastic nanocomposites such as ABS,[61] PS[9] and PMMA[42,43] and other thermoplastic systems in the nanocomposite literature. The presence of dominating PS phase is responsible for the brittleness of the PPO/PS blend. Addition of clay to the blend matrix reduces the break strain by providing resistance to the elongation. The cloisite 10A organoclay leads to a significant reduction in the break strain, possibly due to the presence of the excess organic modifier.

Conclusions

PPO/PS blend nanocomposites were prepared by melt-mixing method with commercially available unmodified Na^+-MMT and organically modified MMT clays Cloisite 10A, Cloisite 30B and Cloisite 20A. These were characterized for structure (WAXD and TEM), thermal behavior (DSC and TGA) and mechanical properties (tensile tests). XRD showed the formation of intercalated nanocomposites for the systems based on Na^+MMT as well as organically modified clays. The Δd_{001} change was in the range of 0.9–1.5 nm for the organically modified clays depending on the chemical nature of the organic modifier, while that observed for Na^+MMT was only one molecular diameter of 0.2 nm. The T_g was not affected significantly. The thermal degradation stability of the blend matrix was found to improve slightly for some systems in the presence of clay layers. The onset of thermal degradation (T_5) showed an increase. No particular trend was observed as a function of the type of organic modification.

The PPO/PS systems prepared with Na-MMT and Cloisite 30B organoclay show a significant retention of tensile strength and break strain elongation. The composites showed improved modulus (upto 35% seen for Cloisite 20A-based system) as compared to the polymer matrix. The hybrids based on unmodified Na-MMT and Cloisite 30B (containing polar hydroxyl groups) showed good retention of tensile strength up to a significant clay loading level. The tensile strength (i.e. break-stress) is not depreciated significantly by the presence and distribution of clay platelets, in case of Cloisite 30B nanocomposites and the Na-MMT-based composites over 2–10 wt% clay loading range. Cloisite 10A organoclay containing excess organic modifier above the stoichiometric

ratio in the MMT leads to a greater reduction in the tensile strength and the break strain of the nanocomposite, despite providing a similar level of increase in the tensile modulus as compared to the other organoclays. The observed behavior of modulus, strength and elongational break strain (which gives some measure of ductility) is found to be useful from a practical standpoint.

Acknowledgments

The authors thank the Council of Scientific and Industrial Research (CSIR), India, for providing a Graduate Senior Research Fellowship for unrestricted research (to RRT) and appreciate the availability of excellent experimental facilities in the Division of Polymer Science and Engineering and in the Center for Materials Characterization (CMC) at the National Chemical Laboratory, Pune; the authors also thank Southern Clay Products, Inc., Texas, and appreciate the provision of the clay samples.

Funding

This research received no specific grant from any funding agency in the public, commercial, or not-for-profit sectors.

References

1. Alexandre M and Dubois P. Polymer-layered silicate nanocomposites: preparation, properties and uses of a new class of materials. *Materials Science and Engineering: R: Reports* 2000; 28 (1-2): 1–63.
2. Giannelis EP. Polymer layered silicates nanocomposites. *Advanced Materials* 1996; 8(1): 29–35.
3. Giannelis EP, Krishnamoorti R and Manias E. Polymer-silicate nanocomposites: Model systems for confined polymers and polymer Brushes. *Advances in Polymer Science* 1999; 138: 107–147.
4. LeBaron PC, Wang Z and Pinnavaia T.J. Polymer-layered Silicate Nanocomposites: an overview. *Applied Clay Science,* 1999; 15(1-2): 11–29.
5. Biswas M and Ray SS. Recent progress in synthesis and evaluation of polymer-montmorillonite nanocomposites. *Advances in Polymer Science* 2001; 155: 167–221.
6. Kojima Y, Usuki A, Kawasumi M, Okada A, Fukushima Y, Karauchi T and Kamigaito O. Synthesis of nylon 6-clay hybrid by montmorillonite intercalated with ε-caprolactam. *Journal of Polymer Science Part A: Polymer Chemistry* 1993; 31: 9838211;986.
7. Kumar S, Jog JP and Natarajan U. Preparation and characterization of poly(methyl methacrylate)–clay nanocomposites via melt intercalation: The effect of organoclay on the structure and thermal properties. *Journal of Applied Polymer Science* 2003; 89(5): 1186–1194.
8. Vaia RA and Giannelis EP. Polymer melt intercalation in organically-modified layered silicates: Model predictions and experiment. *Macromolecules* 1997; 30: 8000–8009.
9. Tanoue S, Utracki LA, Rejon A.R, Tatibouët J and Kamal MR. Melt compounding of different grades polystyrene with organoclay. Part 3: Mechanical properties. *Polymer Engineering and Science* 2005; 45: 827–837.
10. Fornes TD, Yoon PJ, Hunter DL, Keskkula H and Paul DR. Effect of organoclay structure on nylon 6 nanocomposite morphology and properties. *Polymer* 2002; 43: 5915–5933.
11. Yoon PJ, Hunter DL and Paul DR. Polycarbonate nanocomposites. Part 1. Effect of organoclay structure on morphology and properties. *Polymer* 2003; 44: 5323–5339.

12. Lim SK, Kim JW, Chin I, Kwon YK and Choi HJ. Montmorillonite nanocomposite with miscible polymer blend of poly(ethylene oxide) and poly(methyl methacrylate). *Chemistry of Materials* 2002; 14: 1989–1994.
13. Tjong SC, Meng YZ and Xu Y. Preparation and properties of polyamide 6/polypropylene–vermiculite nanocomposite/polyamide 6 alloys. *Journal of Applied Polymer Science* 2002; 86: 2330–2337.
14. Gelfer MY, Song HH, Liu L, Hsiao BS, Chu B, Rafailovich M, Si M and Zaitsev V. Effects of organoclays on morphology and thermal and rheological properties of polystyrene and poly(-methyl methacrylate) blends. *Journal of Polymer Science Part B: Polymer Physics* 2003; 41: 44–54.
15. Moussaif N and Groeinckx G. Nanocomposites based on layered silicate and miscible PVDF/PMMA blends: melt preparation, nanophase morphology and rheological behaviour. *Polymer* 2003; 44: 7899–7906.
16. Chow WS, Ishak M, Kocsis KJ, Apostolov AA and Ishiaku US. Compatibilizing effect of maleated polypropylene on the mechanical properties and morphology of injection molded polyamide 6/polypropylene/organoclay nanocomposites. *Polymer* 2003; 44: 7427–7440.
17. Mehrabzadeh M and Kamal MR. Melt Processing of PA-66/Clay HDPE/Clay and HDPE/PA-66/Clay, Polymer Engineering and Science. 2004; 44(5): 1152–1161.
18. Kim HB, Choi JS, Lee CH, Lim ST, Jhon MS and Choi HJ. Polymer blend/organoclay nanocomposite with poly(ethylene oxide) and poly(methyl methacrylate). *European Polymer Journal* 2005; 41: 679–685.
19. Ray SS, Pouliot S, Bousmina M and Utracki LA. Role of organically modified layered silicate as an active interfacial modifier in immiscible polystyrene/polypropylene blends. *Polymer* 2004; 45: 8403–8413.
20. Li Y and Shimizu H. Novel morphologies of poly(phenylene oxide) (PPO)/polyamide 6 (PA6) blend nanocomposites. *Polymer* 2004; 45: 7381–7388.
21. Lee CH, Kim HB, Lim ST, Choi HJ and Jhon MS. Biodegradable aliphatic polyester-poly (epichlorohydrin) blend/organoclay nanocomposites; synthesis and rheological characterization. *Journal of Materials Science* 2005; 40: 3981–3985.
22. Chow WS, Mohd. Ishak ZA, Ishiaku US, Karger KJ and Apostolov AA. The effect of organoclay on the mechanical properties and morphology of injection-molded polyamide 6/polypropylene nanocomposites. *Journal of Applied Polymer Science* 2004; 91: 175–189.
23. Yoo Y, Park C, Lee SG, Cho i.KY, Kim DS and Lee JH. Influence of addition of organoclays on morphologies in nylon 6/LLDPE blends. *Macromolecular Chemistry and Physics* 2005; 206: 878–884.
24. Chow WS, Mohd. Ishak ZA and Kocsis JK. Morphological and rheological properties of polyamide6/poly(propylene)/organoclay nanocomposites. *Macromolecular Materials and Engineering* 2005; 290: 122–127.
25. Li Y and Shimizu H. Co-continuous polyamide 6 (PA6)/acrylonitrile-butadiene-styrene (ABS) nanocomposites. *Macromolecular Rapid Communications* 2005; 26: 710–715.
26. Chow WS, Mohd. Ishak ZA and Kocsis JK. Atomic force microscopy study on blend morphology and clay dispersion in polyamide-6/polypropylene/organoclay systems. *Journal of Polymer Science Part B: Polymer Physics* 2005; 43: 1198–1204.
27. Gahleitner M, Kretzschmar B, Pospiech D, Ingolic E, Reichelt N and Bernreitner K. Morphology and mechanical properties of polypropylene/polyamide 6 nanocomposites prepared by a two-step melt-compounding process. *Journal of Applied Polymer Science* 2006; 100: 283–291.

28. Lee MH, Dan CH, Kim HJ, Cha J, Kim S, Hwang Y and Lee CH. Effect of clay on the morphology and properties of PMMA/poly(styrene-*co*-acrylonitrile)/clay nanocomposites prepared by melt mixing. *Polymer* 2006; 47: 4359–4369.
29. Kontopoulou M, Liu Y, Austin JR and Parent JS. The dynamics of montmorillonite clay dispersion and morphology development in immiscible ethylene–propylene rubber/polypropylene blends. *Polymer* 2007; 48: 4520–4528.
30. Vo LT and Giannelis EP. Compatibilizing poly(vinylidene fluoride)/nylon-6 blends with nanoclay. *Macromolecules* 2007; 40(23): 8271–8276.
31. Tiwari RR, Khilar KC and Natarajan U. New poly(phenylene oxide)/polystyrene blend nanocomposites with clay: Intercalation, thermal and mechanical properties. *Journal of Applied Polymer Science* 2008; 108: 1818–1828.
32. Kusmono Mohd, Ishak ZA, Chow WS, Takeichi T and Rochmadi. Compatibilizing effect of SEBS-g-MA on the mechanical properties of different types of OMMT filled polyamide 6/polypropylene nanocomposites. *Composites Part A: Applied Science and Manufacturing* 2008; 39: 1802–1814.
33. Martins CG, Larocca NM, Paul DR and Pessan LA. Nanocomposites formed from polypropylene/EVA blends. *Polymer* 2009; 50: 1743–1754.
34. Habi A, Djadoun S and Grohens Y. Morphology and thermal behavior of organo-bentonite clay/poly(styrene-*co*-methacrylic acid)/poly(isobutyl methacrylate-*co*-4-vinylpyridine) nanocomposites. *Journal of Applied Polymer Science* 2009; 114: 322–330.
35. Yang Q-Q, Guo Z-X and Yu J. The effect of organo-montmorillonite on the compatibility and properties of nylon 66/polypropylene blend. *Journal of Applied Polymer Science* 2010; 115: 3697–3704.
36. Filippone G, Dintcheva NTz, La Mantia FP and Acierno D. Selective localization of organoclay and effects on the morphology and mechanical properties of LDPE/PA11 blends with distributed and co-continuous morphology. *Journal of Polymer SciencePart B: Polymer Physics* 2010; 48: 600–609.
37. Brandrup J and Immergut EH. *Polymer Handbook*. 3rd ed., Wiley Interscience. New York. 1989.
38. Hammel R, Macknight WJ and Karasz FE. Structure and properties of the system: poly(2,6–dimethyl–phenylene oxide) isotactic polystyrene. Wide–angle x–ray studies. *Journal of Applied Physics*, 1975; 46: 4199–4203.
39. Runt JP. Polymer blends containing isotactic polystyrene: Thermal behavior of model systems. *Macromolecules* 1981; 14: 420–423.
40. Wellinghoff ST, Koenig JL and Baer E. Spectroscopic examination of chain conformation and bonding in poly(phenylene oxide)–polystyrene blends. *Journal of Polymer Science Part B: Polymer Physics* 1977; 15: 1913–1925.
41. Utracki LA. 1988. *Commercial Polymer Blends*. Chapman and Hall, London.
42. Tiwari RR and Natarajan U. Thermal and mechanical properties of melt processed intercalated poly(methyl methacrylate)–organoclay nanocomposites over a wide range of filler loading. *Polymer International* 2008; 57: 738–743.
43. Tiwari RR and Natarajan U. Influence of organic modification on mechanical properties of melt processed intercalated poly (methyl methacrylate)–organoclay nanocomposites. *Journal of Applied Polymer Science* 2007;105: 2433–2443.
44. Yasmin A, Abot JL and Daniel IM. Mechanical and thermoviscoelastic properties of epoxy/clay nanocomposites. *Materials Research Society Symposium Proceedings* 2003; 740: 167–172.

45. Ratanarat K, Nithitanakul M, Martin DC and Magaraphan R. Polymer-silicate nanocomposites: Linear PEO and highly branched dendrimer for organic wastewater treatment. *Reviews on Advanced Materials Science* 2003; 5: 187–192.
46. Carrasco F and Pagès P. Thermogravimetric analysis of polystyrene: Influence of sample weight and heating rate on thermal and kinetic parameters. *Journal of Applied Polymer Science* 1996; 61: 187–197.
47. Wang D, Zhu J, Yao Q and Wilkie CA. A Comparison of Various Methods for the Preparation of Polystyrene and Poly(methyl methacrylate) Clay Nanocomposites. *Chemistry of Materials* 2002; 14: 3837–3843.
48. Doh JG and Cho I. Synthesis and properties of polystyrene-organoammonium montmorillonite hybrid. *Polymer Bulletin* 1998; 41: 511–518.
49. Tanoue S, Utracki LA, Rejon AG, TatibouŠt J, Cole KC and Kamal MR. Melt compounding of different grades of polystyrene with organoclay. Part 1: Compounding and characterization. *Polymer Engineering and Science* 2004; 44: 1046–1060.
50. Panek G, Schleidt S, Mao Q, Wolkenhauer M, Spiess HW and Jeschke G. Heterogeneity of the Surfactant Layer in Organically Modified Silicates and Polymer/Layered Silicate Composites. *Macromolecules*. 2006; 39(6): 2191–2200.
51. Garcia-Lopez D, Gobernado-Mitre I, Fernandez JF, Merino JC and Pastor JM. Influence of clay modification process in PA6-layered silicate nanocomposite properties. *Polymer* 2005; 46(8): 2758–2765.
52. Morgan AB and Harris JD. Effects of organoclay Soxhlet extraction on mechanical properties, flammability properties and organoclay dispersion of polypropylene nanocomposites. *Polymer* 2003; 44(8): 2313–2320.
53. Shah RK, Hunter DL and Paul DR. Nanocomposites from poly(ethylene-*co*-methacrylic acid) ionomers: Effect of surfactant structure on morphology and properties. *Polymer* 2005; 46(8): 2646–2662.
54. Mandalia T and Bergaya F. Organo clay mineral–melted polyolefin nanocomposites Effect of surfactant/CEC ratio. *Journal of Physics and Chemistry of Solids* 2006; 67(4): 836–845.
55. Vaia RA, Sauer BB, Tse OK and Giannelis EP. Relaxations of confined chains in polymer nanocomposites: Glass transition properties of poly(ethylene oxide) intercalated in montmorillonite. *Journal of Polymer Science Part B: Polymer Physics* 1997; 35: 59–67.
56. Li Y and Ishida H. A study of morphology and intercalation kinetics of polystyrene–organoclay nanocomposites. *Macromolecules* 2005; 38 (15). 6513–6519.
57. Jin HS and Chang JH. Polystyrene nanocomposites via *In-situ* intercalated free radical polymerization, *Fibers and Polymers*, 2007; 8: 451–455.
58. Zheng C and Lee LJ. Poly(methyl methacrylate) and Polystyrene/Clay Nanocomposites Prepared by in-Situ Polymerization. *Macromolecules* 2001; 34: 4098–4103.
59. Zhu J, Morgan AB, Lamelas FJ and Wilkie CA. Fire Properties of Polystyrene–Clay Nanocomposites. *Chemistry of Materials* 2001; 13: 3774–3780.
60. Stretz HA, Paul DR and Cassidy PE. Poly(styrene-*co*-acrylonitrile)/montmorillonite organoclay mixtures: a model system for ABS nanocomposites. *Polymer* 2005; 46: 3818–3830.
61. Stretz HA, Paul DR, Li R, Keskkula H and Cassidy PE. Intercalation and exfoliation relationships in melt-processed poly(styrene-*co*-acrylonitrile)/montmorillonite nanocomposites, *Polymer* 2005; 46(8): 2621–2637.
62. Tiwari RR and Natarajan U. Effect of blend composition and organoclay loading on the nanocomposite structure and properties of miscible poly(methyl methacrylate)/poly(styrene-*co*-acrylonitrile) blends. *Polymer Engineering and Science* 2011; 51: 979–991.

63. Bigg DM. Mechanical properties of particulate filled polymers. *Polymer Composites* 1987; 8: 115–122.
64. Leong YW, Abu Bakar MB, Mohd. Ishak ZA, Ariffin A and Pukanszky B. Comparison of the mechanical properties and interfacial interactions between talc, kaolin, and calcium carbonate filled polypropylene composites. *Journal of Applied Polymer Science* 2004; 91: 3315–3326.
65. Dong Y and Bhattacharyya D. Mapping the real micro/nanostructures for the prediction of elastic moduli of polypropylene/clay nanocomposites. *Polymer* 2010; 51(3): 816–824.
66. Dong Y and Bhattacharyya D. Dual role of maleated polypropylene in processing and material characterisation of polypropylene/clay nanocomposites. *Materials Science and Engineering: A* 2010; 527(6): 1617–1622.